Molecular Vision 2018; 24:340-352 <http://www.molvis.org/molvis/v24/340>
Received 19 December 2017 | Accepted 24 April 2018 | Published 26 April 2018

Placental growth factor promotes epithelial-mesenchymal transition-like changes in ARPE-19 cells under hypoxia

Yi Zhang, Lin Zhao, Lijun Wang, Xiting Yang, Aiyi Zhou, Jianming Wang

Department of Ophthalmology, the Second Affiliated Hospital of Xi'an Jiaotong University

Purpose: To investigate the role of placental growth factor (PGF) in the epithelial-mesenchymal transition (EMT) of ARPE-19 cells under hypoxia, and whether the NF-κB signaling pathway is involved in this process.
Methods: ARPE-19 cells were treated in five groups: a control group, hypoxia group, PGF group, hypoxia+PGF group, and NF-κB-blocked group. A chemical hypoxia model was established in the ARPE-19 cells by adding $CoCl_2$ to the culture medium. The morphological changes after treatment were observed. The proliferation rates were measured with 3-(4,5-dimethyl-2-thiazolyl)-2,5-diphenyl-2H-tetrazolium bromide (MTT) assay. The migration abilities were measured with scratch assay. The EMT biomarkers were measured with quantitative real-time PCR (qRT-PCR), western blotting, and immunofluorescence. The relative protein expression of components of the NF-κB signaling pathway was measured with western blotting and immunofluorescence.
Results: Cells treated with PGF under hypoxia exhibited morphological changes consistent with the transition from an epithelial to a mesenchymal phenotype. In the ARPE-19 cells, exogenous PGF under hypoxia increased the proliferation rate compared to the rate under hypoxia alone ($p<0.05$) and increased the migration rate ($p<0.05$). Treatment of hypoxia-exposed cells with PGF caused decreased expression of the epithelial biomarkers E-cadherin and ZO-1 (both $p<0.05$) and increased expression of the mesenchymal marker α-SMA ($p<0.05$) by enhancing the phosphorylation of NF-κB p65 of the total protein, promoting the translocation of p65 to the nucleus, and inducing the degradation of IκB-α (a negative regulator of the NF-κB pathway) in the ARPE-19 cells. Additionally, the effect of PGF-induced EMT in the ARPE-19 cells under hypoxia was counteracted with BAY 11-7082 (a selective NF-κB inhibitor).
Conclusions: Exogenous PGF promotes EMT-like changes in ARPE-19 cells under hypoxia by activating the NF-κB signaling pathway. The study results suggest that PGF may play a role in scar formation in neovascular age-related macular degeneration (AMD) and that the inhibition of PGF may be a promising target for the prevention and treatment of AMD.

Choroidal neovascularization (CNV) is an important pathologic component of neovascular age-related macular degeneration (AMD), and CNV lesions may progress to an end-stage fibrous plaque or disciform scar, which contributes to the loss of central vision [1]. Hypoxia is essential for the pathogenesis of AMD [2].

Recently, intravitreal injection of antivascular endothelial growth factor (VEGF) drugs has become the main approach for the clinical treatment of CNV [3-5]. However, even with standardized and repeated anti-VEGF treatment, only 30–40% of patients with exudative AMD demonstrate vision improvement [6]. One reason for unsuccessful outcomes that has been identified is the subretinal fibrosis that may develop in approximately half of all anti-VEGF-treated eyes within 2 years [7]. Thus, therapeutic strategies for the inhibition of subretinal fibrosis have become a research hotspot.

Fibrosis is considered to represent an excessive wound healing response to tissue damage [8]. In neovascular AMD, CNV develops in the subretinal and/or subpigment epithelial space, leading to hemorrhage and exudative change and culminating in subretinal fibrosis [9]. Generally, after epithelial cell injury, cells undergo epithelial-mesenchymal transition (EMT), which enables transdifferentiation and results in the conversion of epithelial cells to myofibroblasts [10]. In the healthy eye, the RPE is a highly polarized monolayer of pigmented cells [11] that retain a mature epithelial phenotype and are mitotically quiescent with cell–cell contact inhibition mediated by the homotypic adhesion of cadherins on adjacent cells [12]. Once these contacts are disrupted, RPE cells lose their epithelial phenotype, with decreasing expression of epithelial markers, such as E-cadherin and ZO-1, and gain mesenchymal properties, with increasing expression of mesenchymal markers, such as N-cadherin, vimentin, and α-SMA [10]. RPE could be the origin of myofibroblastic cells through the development of EMT [13]. Thus, the EMT of RPE cells is a critical step in subretinal fibrosis.

Placental growth factor (PGF) is a member of the VEGF family and specifically binds to the receptor VEGFR-1 [14-16]. PGF is known to stimulate the growth, migration, and survival of endothelial cells [17,18]. Unlike VEGF expression,

Correspondence to: Jianming Wang, Department of Ophthalmology, the Second Affiliated Hospital of Xi'an Jiaotong University, Xi'an, Shaanxi 71000, P. R. China, Phone: +86-18991237392; FAX: +86-029-87679449; email: xajdwjm@163.com

PGF levels are low or undetectable in healthy tissue but are increased in disease settings [19,20]. Potential involvement of PGF has been described in wound healing, collateral vessel formation in ischemia, and tumor growth [21,22]. Literature concerning the role of PGF in retinal pathology is sparser, although it has been reported that mice lacking PGF show less neovascularization after laser treatment [23]. Another group demonstrated similar results after pharmacologic blockade of PGF [24]. Extracellular hypoxia produced additive PGF gene expression [25]. Our previous study found that PGF expression is iatrogenically upregulated by anti-VEGF therapy [26]. Emerging evidence suggests that PGF is a key regulatory factor involved in controlling angiogenic and inflammatory responses and pathological angiogenesis, especially in retinal disorders. In recent years, PGF has been demonstrated to play an important role in triggering EMT in hyperoxia-induced acute lung injury [27,28], cervical cancer [29], and breast cancer [30]. However, whether PGF promotes epithelial-mesenchymal transition-like changes in subretinal fibrosis of neovascular AMD has not been reported, and the possible molecular mechanisms underlying the process have not been elucidated.

Thus, in the present study, we investigated the role of PGF in the EMT of ARPE-19 cells under hypoxia. Moreover, we demonstrated that the NF-κB signaling pathway could regulate this process.

METHODS

Cell culture and treatment: The human RPE cell line ARPE-19 was obtained from the American Type Culture Collection (ATCC, Manassas, VA) and maintained in Dulbecco's modified Eagle's medium/F-12 HAM (DMEM/F-12, HyClone, Logan, UT) containing 10% fetal bovine serum (FBS, Gibco, South America) and 1% penicillin and streptomycin (Life Technologies, Grand Island, NY) under a humidified atmosphere containing 5% CO_2 at 37 °C. The medium was changed every 2–3 days. Cells were routinely passaged at 80% to 90% confluence and a split ratio of 1:3 by digestion in 0.25% trypsin-ethylene diamine tetraacetic acid (HyClone). Semiconfluent cultures (70–80% confluency) were serum starved for 24 h, and after starvation, the cells were treated as described below. The 3-(4,5-dimethyl-2-thiazolyl)-2,5-diphenyl-2H-tetrazolium bromide (MTT) assay comprised three subassays. In the first assay, cells were treated with different doses of $CoCl_2$ (0, 25, 50, 100, 200, 400, and 800 μM) for 12 h; in the second assay, the cells were treated with different doses of PGF (0, 12.5, 25, 50, 100, 200, and 400 ng/ml) for 48 h; and in the third assay, the cells were first treated with 200 μM $CoCl_2$ for 12 h and then with different doses of PGF (0, 25, 100, and 400 ng/ml) for 48 h, with the exception of the control group, which received neither $CoCl_2$ treatment nor PGF treatment. In the other assays, the cells were treated as follows: The control group was cultured with cell culture medium containing 1% FBS (control); the hypoxia group was cultured with 200 μM $CoCl_2$ (Sigma Aldrich, St. Louis, MO) dissolved in medium containing 1% FBS for 12 h (hypoxia); the PGF group was cultured with 100 ng/ml PGF (R&D Systems, Minneapolis, MN) dissolved in medium containing 1% FBS for 48 h (PGF); the hypoxia+PGF group was cultured with 200 μM $CoCl_2$ for 12 h and then cultured with 100 ng/ml PGF for 48 h (hypoxia+PGF); and the NF-κB signaling pathway-blocked group was first cultured with 200 μM $CoCl_2$ for 12 h and then treated with 2 μM Bay 11-7082 (Sigma) for 30 min before culture with 100 ng/ml PGF for 48 h (NF-κB blocking).

Cell authentication: Short tandem repeat (STR) analysis was used to validate the ARPE-19 cells used in this study. Nineteen short tandem repeat (STR) loci plus the gender determining locus, amelogenin, were amplified using the commercially available EX20 Kit from AGCU (Wuxi, China). The cell line sample was processed using the ABI Prism® 3500 Genetic Analyzer. Data were analyzed using GeneMapper® ID-X v1.4 software (Applied Biosystems, Suzhou, China). Appropriate positive and negative controls were run and confirmed for each sample submitted. The STR analyses are presented in Appendix 1.

Morphological observation: The morphological characteristics of the cells after treatment were observed. We collected images at 100X magnification on an inverted phase contrast microscope (Nikon Eclipse TS100, Nikon, Tokyo, Japan) after appropriate treatments.

MTT assay: Cultured ARPE-19 cells after 48 h of treatment with different doses of PGF with or without hypoxia pretreatment were assayed for viability using the MTT assay. Cells were seeded into 96-well plates at 4×10^3 cells/well. After incubation with the indicated concentrations of PGF for 48 h with or without pretreatment with 200 μM $CoCl_2$ for 12 h, the MTT solution (5 mg/ml, Sigma-Aldrich) was added to each well and incubated for 4 h at 37 °C. Then the supernatant was discarded, and 150 μl dimethyl sulfoxide (DMSO, Sigma) was administered for 10–15 min. The absorbance was recorded at 570 nm with a Microplate Reader (BioTek, PowerWave XS, Winooski, VT). The experiment was executed in triplicate and represented graphically as a percentage of the proliferation rate.

Scratch assay: Cell density was adjusted to 1×10^7 cells/ml, and 2 ml of cell suspension was added to each well of a premarked 6-well plate. When the cells reached confluence,

two straight parallel lines were scratched into the cell layers in each well using a sterile 10 µl pipette tip. Thereafter, cellular debris were washed away with PBS (1X; 137 mM NaCl,2.7 mM KCl,10 mM Na_2HPO_4,2 mM KH_2PO_4, pH 7.4), the medium for each group was added, and photographs were taken at selected regions at 100X magnification under an inverted phase contrast microscope (Nikon Eclipse TS100). After incubation for another 12 h, pictures were taken again at the same regions. The experiments were repeated three times. For further quantitative analyses, the gap size of the wound was measured using ImageJ software (National Institutes of Health, Bethesda, MD), and the percentage coverage of the wound was evaluated as the migration rate.

RNA isolation and qRT-PCR: Total RNA was isolated using TRIzol (Invitrogen, Carlsbad, CA) according to the manufacturer's instructions. Total RNA was reverse-transcribed using the PrimeScript™ RT Master Mix (Takara, Dalian, China). The following conditions were used: 15 min at 37 °C, and then 5 s at 85 °C and then holding at 4 °C. Quantitative real-time PCR (qRT-PCR) was performed using SYBR Premix Ex Taq™ II (Takara). Quantitative PCR was performed in an ABI StepOne (Applied Biosystems, Grand Island, NY) instrument. The amplification program performed by the manufacturer's instructions, as follows: 30 s at 95 °C, and then 40 cycles of 5 s at 95 °C and 30 s at 60 °C. Relative gene expression levels were normalized to β-actin levels and calculated using the comparative Ct ($2^{-\Delta\Delta Ct}$) method. The sequences of the primers used are as follows: α-SMA, forward: 5′-CCG ACC GAA TGC AGA AGG A-3′, reverse: 5′-ACA GAG TAT TTG CGC TCC GAA-3′; ZO-1, forward: 5′-AGC CAT TCC CGA AGG AGT TGA G-3′, reverse: 5′-ATC ACA GTG TGG TAA GCG CAG C-3′; β-actin, forward: 5′-TCC CTG GAG AA GAG CTA CGA-3′, reverse: 5′-AGC ACT GTG TTG GCG TAC AG-3′.

Immunofluorescence: The ARPE-19 cells were seeded on glass coverslips at a density of 5×10^4 cells per well in 24-well culture plates. After the appropriate culture time, the cells were fixed with 4% formaldehyde in PBS for 15 min at room temperature, followed by permeabilization with 0.1% Triton X-100 in PBS for 15 min. After blocking with normal goat serum working solution for 20 min, the cells were incubated with α-SMA primary antibody (1:100 dilution; Abcam, Cambridge, UK) and p65 (1:50 dilution; Cell Signaling Technology, Beverly, MA) overnight. After washing with PBS, fluorescein isothiocyanate (FITC)-conjugated goat anti-rabbit secondary antibody was added and incubated for 1 h in the dark. Cells were washed and then incubated for 10 min with 4′,6-diamidino-2-phenylindole (DAPI; Vector Laboratories, Burlingame, CA) to stain the nuclei. Images were captured using a fluorescence microscope (Nikon Eclipse Ti-E) at 200X magnification. Images were processed in ImageJ.

Western blotting: The protein expression in the ARPE-19 cells was measured with western blotting. Briefly, after washing twice with PBS, the cultured cells were collected and lysed in ice-cold radioimmunoprecipitation assay (RIPA) buffer containing protease inhibitors (Roche, Indianapolis, IN) and the phosphatase inhibitor phosSTOP (Roche). The nuclear and cytosolic proteins were extracted using a nuclear and cytoplasmic protein extraction kit (CWBiotech, Beijing, China) according to the manufacturer's protocol. The lysates were centrifuged at 15,000 ×*g* for 15 min at 4 °C. Protein concentration was measured using a standard bovine serum albumin (BSA) curve. Samples containing equal amounts of protein (60 µg) were separated by sodium dodecyl sulfate–polyacrylamide gel electrophoresis (SDS–PAGE) and transferred to polyvinylidene difluoride (PVDF) membranes (Millipore, Bedford, MA). Nonspecific binding of the membranes was blocked with blocking buffer (5% non-fat skim milk/1× TBS/0.1% Tween-20) for 1 h at room temperature. The membranes were hybridized with the appropriate dilution of a specific primary antibody (E-cadherin, Abcam, 1:1,000; α-SMA, Abcam, 1:10,000; β-actin, Proteintech (Chicago, IL), 1:5,000; p65, CST (Beverly, MA), 1:1,000; phospho-p65 (p-p65), CST, 1:1,000; IκB-α, CST, 1:1,000; histone H3, CST, 1:1,000) overnight at 4 °C and then washed three times before incubating with horseradish peroxidase (HRP)-conjugated secondary antibodies at the appropriate dilution for 1 h at room temperature. The bands were visualized with an enhanced chemiluminescence (ECL) HRP substrate (Millipore) using a chemiluminescence imaging system (Syngene G:BOX Chemi HR16; Syngene, Frederick, MD). β-actin served as a total and cytosolic internal reference, and histone H3 served as a nuclear internal reference.

Statistical analysis: The data are shown as the mean ± standard deviation (SD), analyzed using SPSS 13.0 (SPSS Inc., Chicago, IL) for Windows. Differences among three or more groups were analyzed with one-way ANOVA (ANOVA). A p value of less than 0.05 was considered statistically significant.

RESULTS

Effects of exogenous PGF on morphological changes of ARPE-19 cells under hypoxia: ARPE-19 is a human RPE cell line with an epithelial morphology. To observe the effects of exogenous PGF on morphological changes of ARPE-19 cells under hypoxia, we took photos after the treatments (Figure 1). The results showed that the control group maintained the morphological characteristics of epithelial cells, exhibiting a cobblestone-like epithelial morphology with a relatively

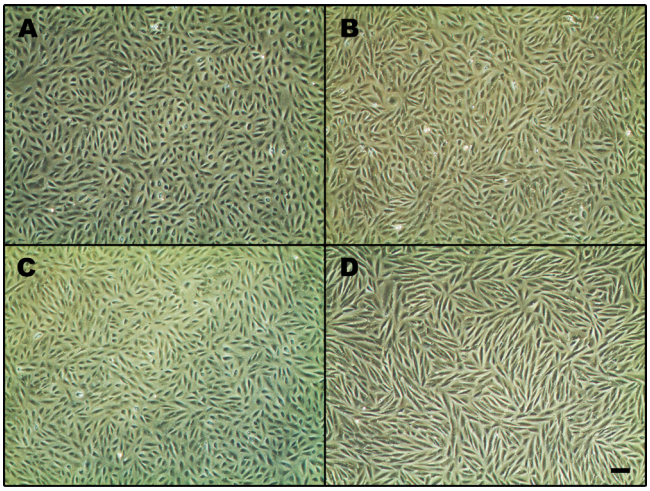

Figure 1. Effects of exogenous PGF on morphological changes of ARPE-19 cells under hypoxia. **A**: The control group exhibited a cobblestone-like epithelial morphology. The hypoxia group (**B**) and the placental growth factor (PGF) group (**C**) did not show obvious morphological differences compared with the control group. **D**: After treatment, cells in the hypoxia+PGF group exhibited a marked transition to a more elongated spindle-like mesenchymal morphology and were arranged in a disorderly fashion compared with the cells in the control group (**A**), the hypoxia group (**B**), and the PGF group (**C**). Scale bar: 200 μM.

neat arrangement. The cells treated with PGF under hypoxia showed obvious changes in cell morphology, presenting with a marked transition from an epithelial to a mesenchymal phenotype; the cells adopted a more elongated spindle-like morphology and were arranged in a disorderly way. No obvious morphological changes were observed in the cells subjected to hypoxia alone or treated with PGF alone.

Effects of exogenous PGF on proliferation of ARPE-19 cells under hypoxia: The viability of the ARPE-19 cells was measured with MTT assays. The cell proliferation rate was decreased considerably under hypoxia induced by $CoCl_2$. Exogenous PGF alone did not influence the proliferation rate of the cells. However, exogenous PGF increased the proliferation rate of the ARPE-19 cells under hypoxia compared to the cells under hypoxia alone (Figure 2).

Effects of exogenous PGF on migration in ARPE-19 cells under hypoxia: The scratch assay was used to measure the effects of exogenous PGF on the migration of the ARPE-19 cells under hypoxia. The ARPE-19 cells treated with PGF and hypoxia exhibited statistically significantly increased migration compared with the control, hypoxia alone, and PGF alone groups ($p<0.05$). Treatment with hypoxia alone or PGF alone exerted no apparent influence on the migration ability of the ARPE-19 cells (Figure 3).

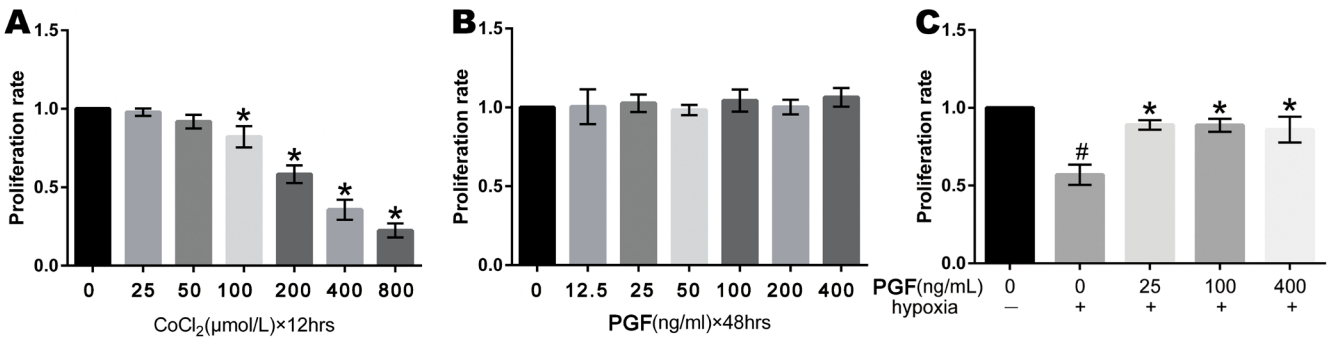

Figure 2. Effects of hypoxia and PGF on the proliferation of ARPE-19 cells. **A**: Hypoxia exposure decreased the proliferation rate of ARPE-19 cells, *$p<0.05$ versus the control group. **B**: Exogenous placental growth factor (PGF) did not affect the proliferation rate of the ARPE-19 cells. **C**: Exposure to hypoxia (treatment with $CoCl_2$ for 12 h) and the addition of exogenous PGF for 48 h increased the proliferation rate of the ARPE-19 cells; *$p<0.05$ versus the hypoxia group (treatment of $CoCl_2$ for 12 h). Exposure to hypoxia decreased the proliferation rate of the ARPE-19 cells; #$p<0.05$ versus the control group. Data are the mean ± standard deviation (SD) of three independent experiments.

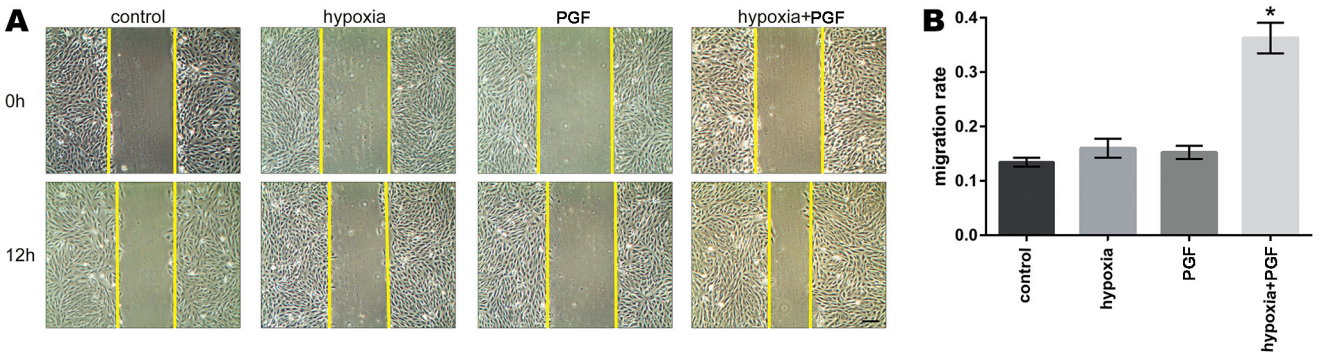

Figure 3. Effects of exogenous PGF on migration in ARPE-19 cells under hypoxia. **A**: Treatment with hypoxia alone or placental growth factor (PGF) alone did not affect the migration rate in the ARPE-19 cells compared with the control treatment, but the hypoxia+PGF treatment increased the migration rate in the ARPE-19 cells compared with the other three treatments. **B**: Quantitative analysis of the migration rates of the different groups is shown in the bar graph. Migration rate = [scratched area (0 h) – scratched area (12 h)] / scratched area (0 h). Data are the mean ± standard deviation (SD) of three independent experiments. Scale bar: 200 μM. *p<0.05 versus the other three groups.

Effects of exogenous PGF on EMT in ARPE-19 cells under hypoxia: EMT of the ARPE-19 cells was measured with qRT-PCR, western blotting, and immunofluorescence staining of biomarkers of EMT at the mRNA and protein levels. The results showed that treatment of the hypoxia-exposed cells with PGF caused decreased expression of E-cadherin and ZO-1 (both $p<0.05$), which are epithelial biomarkers, and increased expression of α-SMA ($p<0.05$), a mesenchymal marker, which suggested the occurrence of EMT, but neither exogenous PGF nor hypoxia exposure alone promoted EMT (Figure 4A,B and Figure 5).

PGF stimulates the activation of NF-κB signaling in ARPE-19 cells under hypoxia: To determine whether the NF-κB signaling pathway was activated in the ARPE-19 cells treated with PGF under hypoxia, we first investigated the protein expression of NF-κB-p-p65 and IκB-α with western blotting of the total protein. Then, we examined the protein expression of IκB-α and p-p65 in cytoplasmic protein and p65 and p-p65 in nuclear protein to determine whether p65 is translocated to the nucleus. As shown in Figure 4, the p-p65 levels in the total protein and the cytoplasmic protein were increased in the hypoxia+PGF group compared with the control group, the hypoxia group, and the PGF group ($p<0.05$), and the expression of IκB-α was decreased ($p<0.05$). In the nuclear protein fraction, we found that the expression of p65 and p-p65 in the hypoxia+PGF group was increased compared with that in the control group, the hypoxia group, and the PGF group ($p<0.05$).

The NF-κB inhibitor counteracts the effect of PGF on EMT in ARPE-19 cells under hypoxia: To explore whether the EMT-promoting effect of PGF in ARPE-19 cells under hypoxia was achieved through NF-κB signaling, we treated a group of cells with Bay 11-7082, a specific inhibitor of NF-κB signaling, and then examined the expression of biomarkers related to EMT and NF-κB signaling in total protein and nuclear protein (Figure 6). The results showed that the NF-κB signaling blocking group did not experience the EMT-inducing effect observed in the hypoxia+PGF group. The expression of the α-SMA protein in the NF-κB blocking group was decreased, and the expression of the E-cadherin and ZO-1 proteins was increased, compared to those in the hypoxia+PGF group ($p<0.05$). Additionally, the NF-κB blocking group showed a reversal of the activation of NF-κB signaling through increased expression of IκB-α in the total protein and decreased expression of p65 in the nuclear protein compared to those in the hypoxia+PGF group ($p<0.05$). The immunofluorescence results (Figure 5 and Figure 7) also showed that the increased expression of α-SMA in the hypoxia+PGF group compared with that in the control group, the hypoxia group, and the PGF group ($p<0.05$) was decreased in the NF-κB blocking group ($p<0.05$), and the increased p65 in the nucleus of hypoxia+PGF group was also decreased in the NF-κB blocking group.

DISCUSSION

In the present study, we found that hypoxia plus exogenous PGF treatment changed cell morphological characteristics and promoted cell proliferation compared to hypoxia treatment alone, and promoted the EMT process by stimulating the NF-κB signaling transduction pathway in ARPE-19 cells. However, exogenous PGF alone did not cause these effects in ARPE-19 cells under normal conditions.

In addition to RPE cells, there are many other kinds of cells, such as human retinal endothelial cells (HRECs)

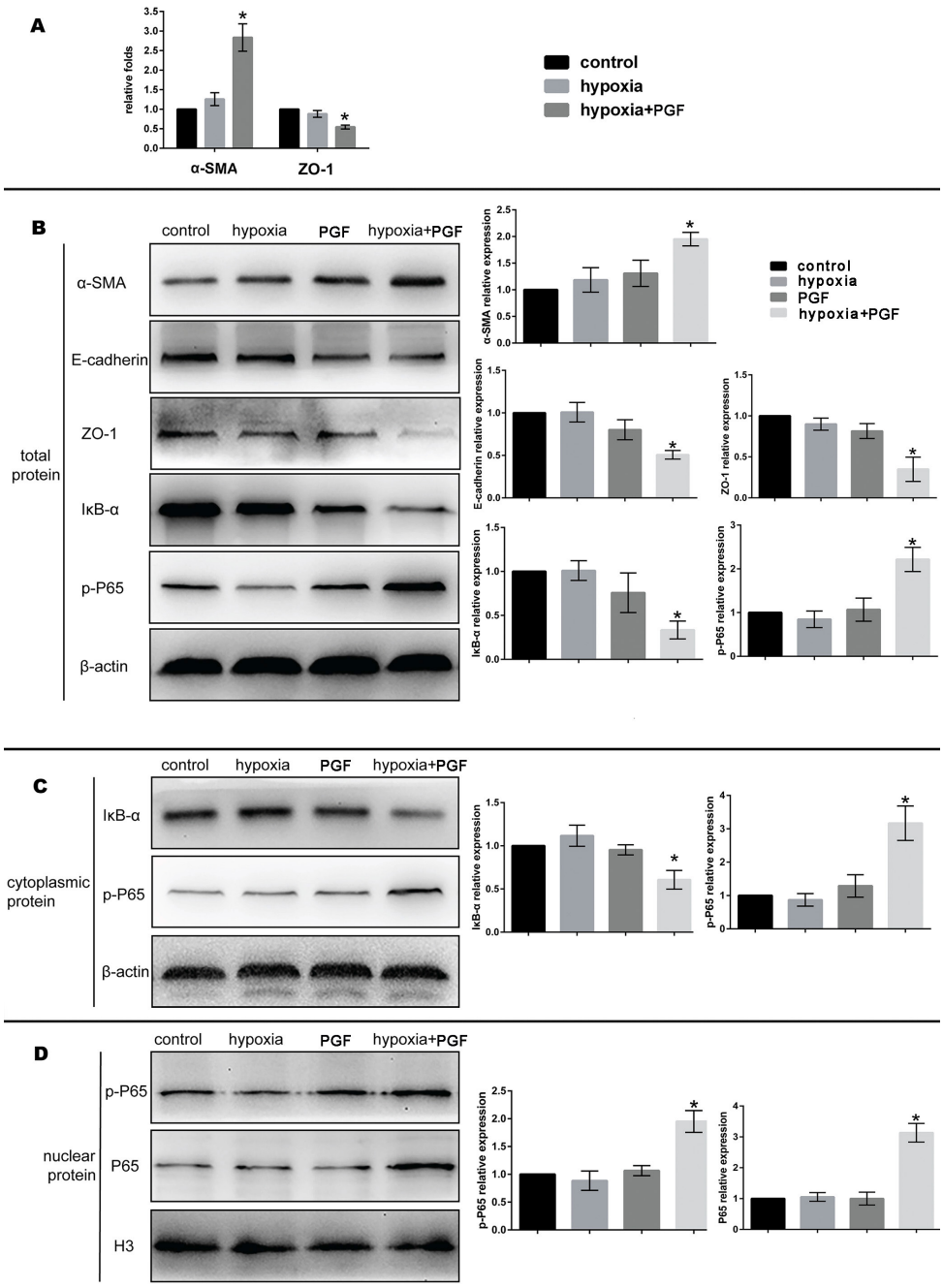

Figure 4. Effects of exogenous PGF on EMT in ARPE-19 cells under hypoxia. **A**: Relative mRNA expression levels of α-SMA and ZO-1 in the control group, the hypoxia group, and the hypoxia+placental growth factor (PGF) group. The relative mRNA expression levels of α-SMA and ZO-1 were increased and decreased, respectively, in the ARPE-19 cells from the hypoxia+PGF group compared with cells from the other two groups (*p<0.05, data are the mean ± standard deviation [SD], n = 3). **B**: Representative protein blots of α-SMA, E-cadherin, ZO-1, IκB-α, and phospho-p65 (p-p65) in the total protein samples and the semiquantitative analyses of the protein expression levels. β-actin was used as the internal reference. **C**: Representative protein blots of IκB-α and p-p65 in the cytoplasmic protein samples and the semiquantitative analyses of the protein expression levels. β-actin was used as the internal reference. **D**: Representative protein blots of p-p65 and p65 in the nuclear protein and semiquantitative analyses of the protein expression levels. Histone H3 was used as the nuclear internal reference. Data are the mean ± standard deviation (SD), n = 3, *p<0.05 versus the other three groups.

[31-33], retinal microglia [34], mononuclear phagocytes (MPs) [35,36], retinal astrocytes [37], and human glial cells [32], that can express the PGF gene in the retinal microenvironment. In this microenvironment containing PGF, RPE cells also respond to the changed PGF under abnormal conditions [38]. The present results indicating PGF alone failed to affect cell proliferation agreed with the results of previous studies [38,39]. As exogenous PGF did not alter the proliferation of ARPE-19 cells, we then explored the effect of PGF on ARPE-19 cells under hypoxia and found that PGF promoted cell proliferation in this group compared to the hypoxia group. Regarding migration, we also found that the hypoxia+PGF group had increased cell migration ability compared with the hypoxia alone or PGF alone groups. Previous studies demonstrated that PGF levels are low or undetectable in healthy tissue but increase in disease settings [19,20]. PGF has been described as potentially involved in pathological angiogenesis and vascular leakage in ischemia, cancer, and wound healing [40]. In other words, PGF is often involved in pathological processes but not in healthy or normal conditions, which can explain the present results regarding the different effects of PGF on cells under normal and hypoxia conditions, to a certain degree.

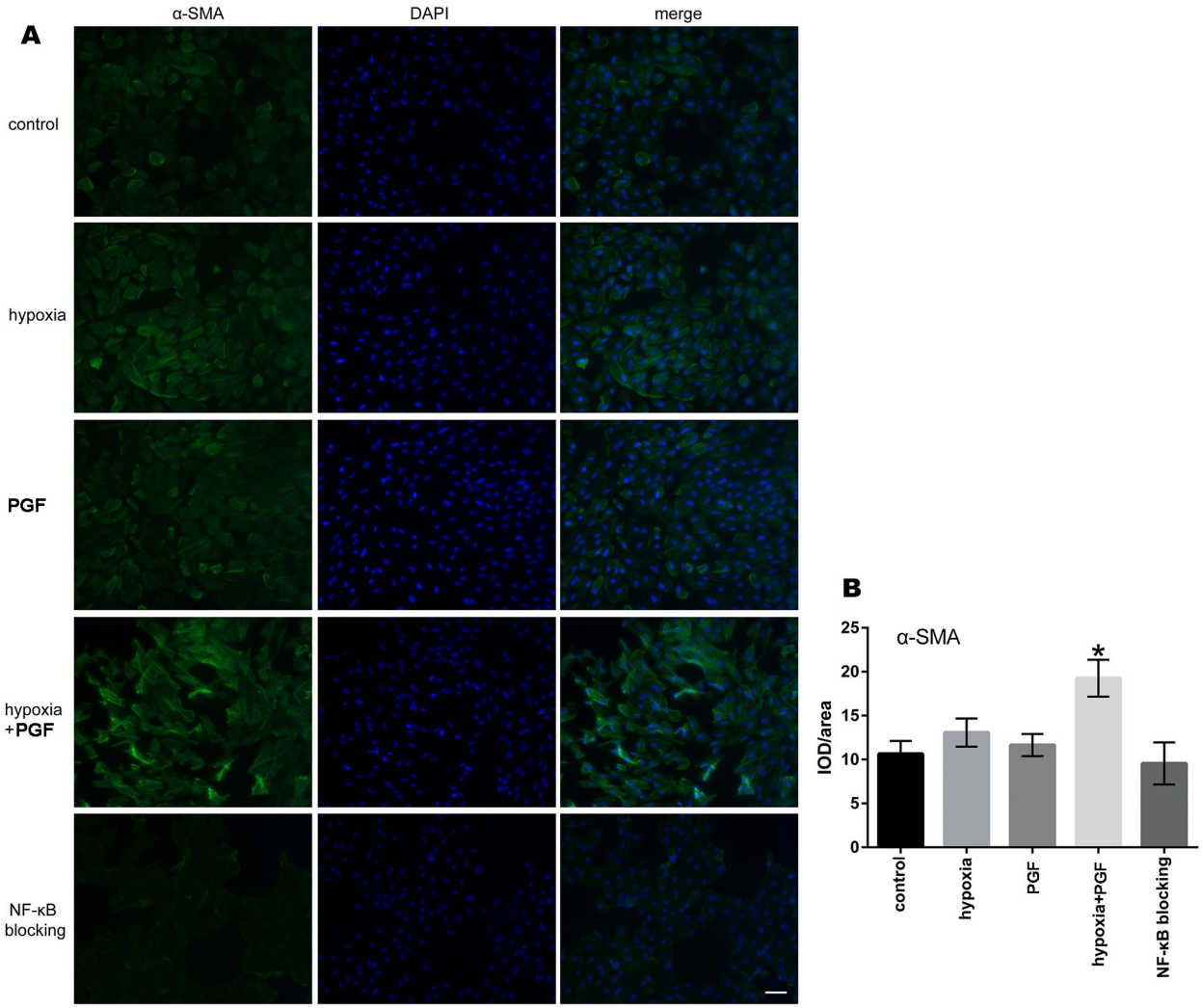

Figure 5. Effects of exogenous PGF on α-SMA expression in ARPE-19 cells under hypoxia. **A**: Representative images of immunofluorescence staining of ARPE-19 cells. Increased expression of α-SMA was observed in ARPE-19 cells from the hypoxia+placental growth factor (PGF) group compared to the control group, the hypoxia group, and the PGF group. Treatment with an NF-κB signaling inhibitor restored this change. Scale bar: 200 μm. **B**: Quantitative analysis of the fluorescence intensity of α-SMA is shown in the bar graph. Data are the mean ± standard deviation (SD), n = 3, *p<0.05 versus the other four groups.

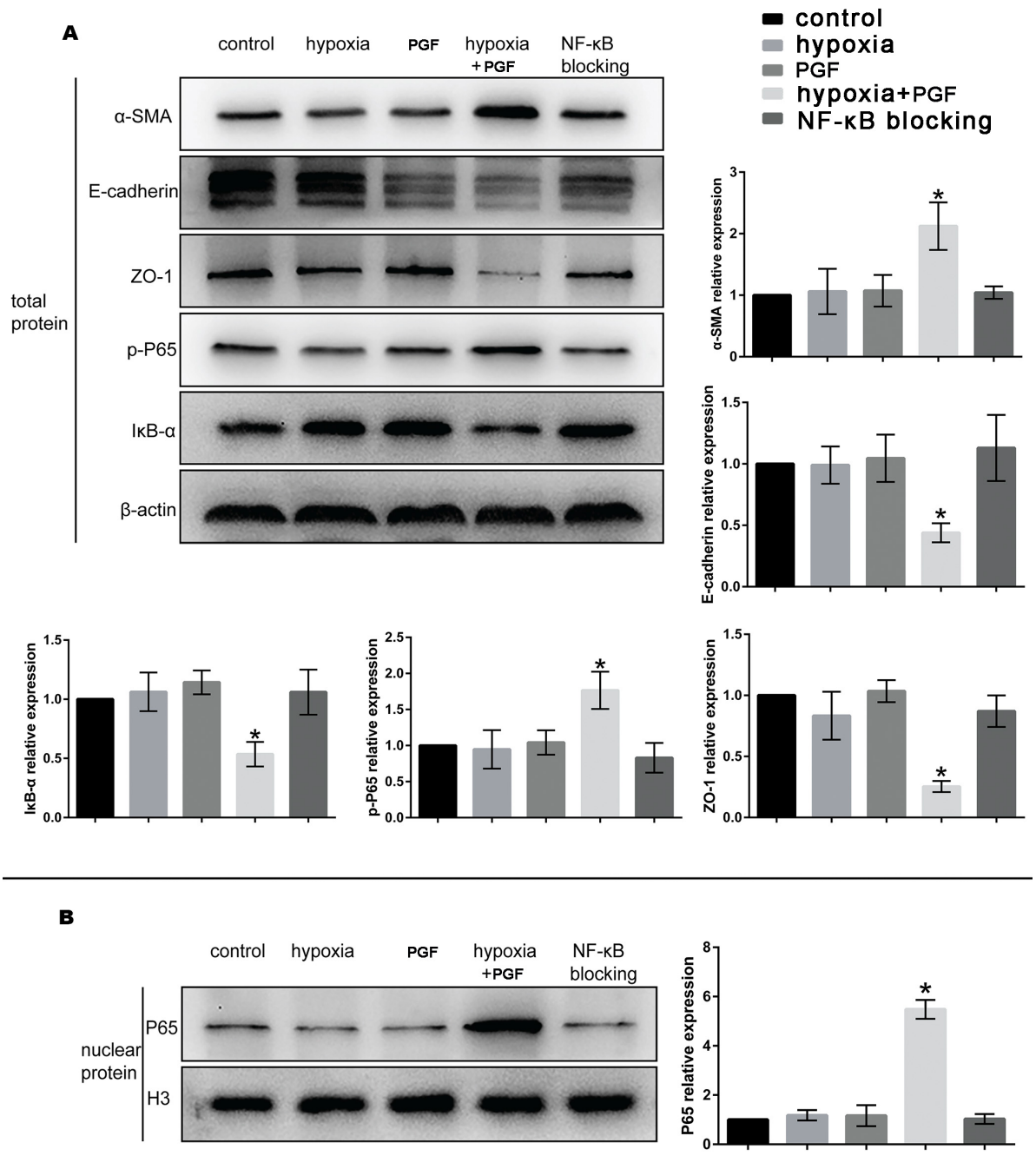

Figure 6. The NF-κB inhibitor counteracts the effect of PGF on the EMT in ARPE-19 cells under hypoxia. **A**: Representative protein blots of α-SMA, E-cadherin, ZO-1, p- p65, and IκB-α in the total protein and semiquantitative analyses of the protein expression levels. β-actin was used as the internal reference. **B**: Representative protein blots of p65 in the nuclear protein and semiquantitative analyses of the protein expression levels. Histone H3 was used as the nuclear internal reference. Data are the mean ± standard deviation (SD), n = 3, *p<0.05 versus the other four groups.

EMT is a biologic process in which epithelial cells lose their epithelial character and gain features of mesenchymal cells [41]. The results of pathology studies have highlighted the role of EMT in the pathogenesis of many fibrotic diseases, such as kidney fibrosis [42,43], hepatic fibrosis [44,45], and intestinal fibrosis [46]. Recent studies have suggested that PGF not only can promote pathological angiogenesis but also can activate the EMT process [26-29]. EMT is also a critical process in subretinal fibrosis in neovascular AMD. Hypoxia plays an important role in the pathogenesis of AMD. However, whether PGF can promote EMT-like changes in ARPE-19 cells under hypoxia has not been reported. The present study explored this question from two perspectives, that of morphological changes and that of the changes to the biomarkers of EMT. Regarding cell morphology, we found that PGF induced a change from the normal morphology to myofibroblast-like morphology and characteristics under hypoxia, but this change did not occur in the ARPE-19 cells treated with hypoxia alone or PGF alone. In terms of EMT biomarkers, the results of the qRT-PCR, western blotting, and immunofluorescence experiments showed that the mesenchymal marker α-SMA was increased in the hypoxia+PGF group at the mRNA and protein levels, and the epithelial markers E-cadherin and ZO-1 were decreased,

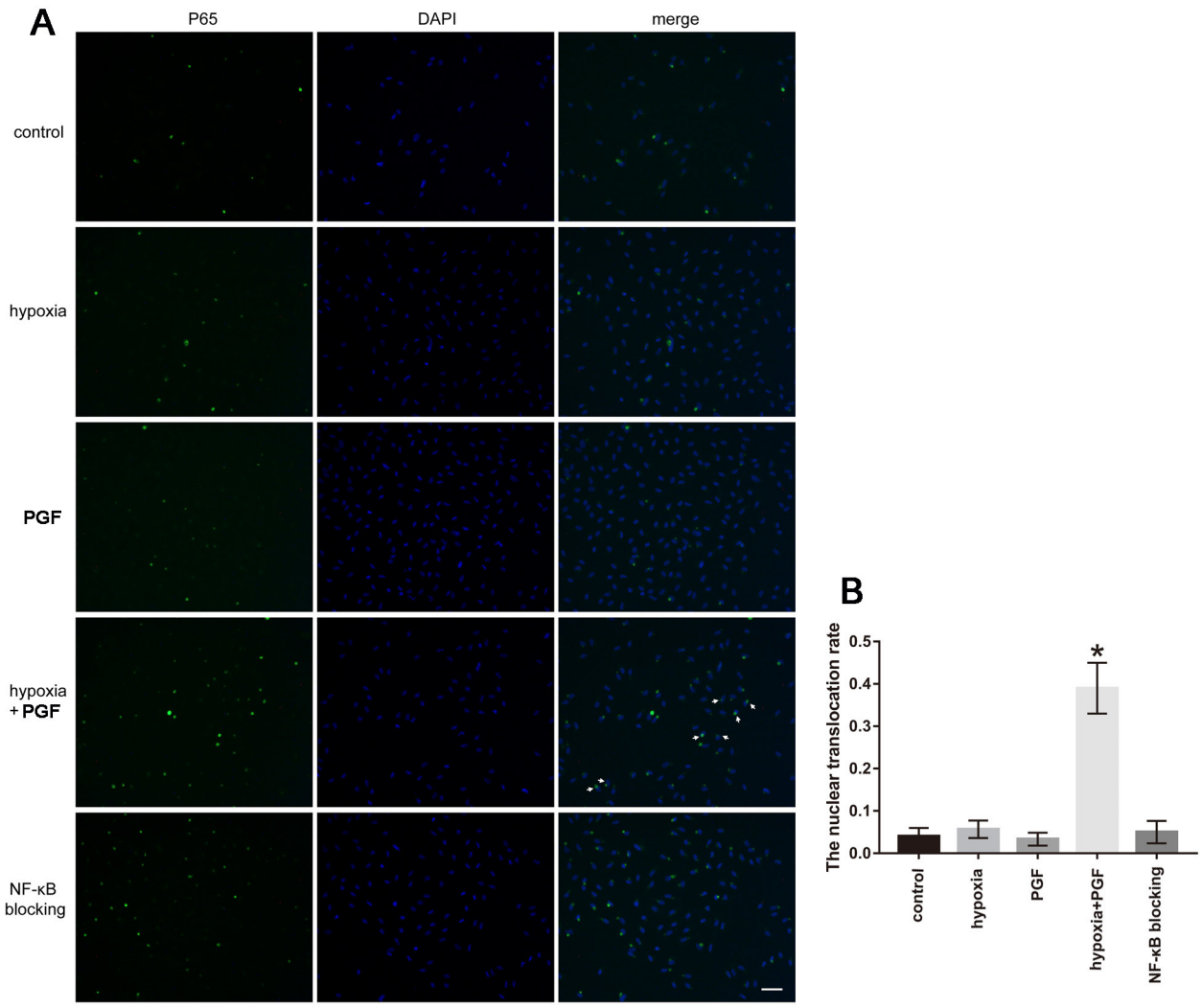

Figure 7. Effects of exogenous PGF on NF-κB p65 expression in ARPE-19 cells under hypoxia. **A**: Increased expression of p65 in the nuclear fraction of ARPE-19 cells was observed in the hypoxia+placental growth factor (PGF) group (as shown with white arrows). Treatment with the NF-κB signaling inhibitor restored this change. Scale bar: 200 µm. **B**: Quantitative analysis of the nuclear translocation rate is shown in the bar graph. Nuclear translocation rate = the number of cells with nuclear immunofluorescence staining / the number of cells with nuclear or cytoplasmic immunofluorescence staining. Data are the mean ± standard deviation (SD), n = 3, *p<0.05 versus the other four groups.

but the hypoxia alone or PGF alone treatments did not induce EMT changes. We hypothesized that the ARPE-19 cells under hypoxia were frailer and thus, damaged and influenced more easily by PGF than normal ARPE-19 cells are. Some slight substructure changes may have occurred in the frailer ARPE-19 cells at first, and then the influence of PGF became obvious enough to promote the EMT changes. That is, hypoxia made the ARPE-19 cells more susceptible to damage than normal cells, and with this background, together with the stimulation of PGF, the damaged ARPE-19 cells were more susceptible to the changes involved in EMT. Together with these findings, these data indicated that PGF promoted EMT-like changes in ARPE-19 cells under hypoxia.

In recent years, the NF-κB signaling pathway, which is considered a canonical inflammation signaling pathway, has been found to play a critical role in liver [47], renal [48], and pulmonary fibrosis [49]. Additionally, it has been demonstrated that the NF-κB signaling pathway is involved in liver and renal fibrosis through activated NF-κB signaling [50,51]. To explore the signaling pathway involved in PGF-induced EMT in ARPE-19 cells under hypoxia, and to further confirm that the PGF-induced EMT-like changes under hypoxia in ARPE-19 cells were associated with activated NF-κB signaling, the relative expression of proteins involved in NF-κB signaling was examined, and BAY 11-7082 (a specific NF-κB inhibitor) was used to suppress NF-κB activity. We found that PGF treatment under hypoxia enhanced the phosphorylation of the p65 total protein, promoted the translocation of p65 to the nucleus, and induced the degradation of IκB-α (a negative regulator of the NF-κB pathway) in ARPE-19 cells. The exogenous PGF-induced reduction of E-cadherin and ZO-1 and the increase in α-SMA under hypoxia were counteracted by BAY 11-7082 as the relevant actors in the activated NF-κB signaling pathway were inhibited. These results suggest that the activation of the NF-κB signaling pathway played an important role in PGF-induced EMT in ARPE-19 cells under hypoxia. As we know, EMT is a complex process that many signaling pathways participate in. In this preliminary study, we chose the NF-κB signaling pathway as the first step because the activation of this signaling pathway is common in the EMT process, and other signaling pathways changed by PGF plus hypoxia in ARPE-19 cells and the interaction between signaling pathways should be investigated in the future.

Although the PCR and western blotting results confirmed the expression of ZO-1 in ARPE-19 cells in this study, the expression may not as sufficient and mature as in cells of post-confluence for several weeks to months, as ARPE-19 cells usually require several weeks to months after reaching confluence to approach an epithelial state. In addition, the experimental analyses of EMT indicators demonstrated the occurrence of EMT in ARPE-19 cells; the possible situation is that PGF stimulation may not be the initiating step of EMT in ARPE-19 cells but just promote the EMT. This situation is similar to that of transforming growth factor β (TGF-β), a well-established EMT inducer of ARPE-19 cells. It has been demonstrated that TGF-β is unable to initiate EMT in cells that maintain well-established cell–cell contact, and disruption of cell–cell contact is a crucial step in initiating EMT [52]. Additional in-depth studies are needed to investigate this issue.

In conclusion, we demonstrated that exogenous PGF promotes EMT-like alterations in ARPE-19 cells under hypoxia by activating the NF-κB signaling pathway. PGF may play a role in scar formation in neovascular AMD, and the inhibition of PGF may be a promising target for the prevention and treatment of AMD.

APPENDIX 1. STR ANALYSIS.

To access the data, click or select the words "Appendix 1"

ACKNOWLEDGMENTS

This study was supported by the key research and development project of Shaanxi Province (2017SF-266). The authors declare no competing financial interests. Dr. Jianming Wang (xajdwjm@163.com) and Dr. Aiyi Zhou (sandy_chow@126.com) are co-corresponding authors on this paper.

REFERENCES

1. Ryan SJ. The development of an experimental model of subretinal neovascularization in disciform macular degeneration. Trans Am Ophthalmol Soc 1979; 77:707-45. [PMID: 94717].
2. Blasiak J, Petrovski G, Veréb Z, Facskó A, Kaarniranta K. Oxidative stress, hypoxia, and autophagy in the neovascular processes of age-related macular degeneration. BioMed Res Int 2014; 2014:768026-[PMID: 24707498].
3. Martin DF, Maguire MG, Ying GS, Grunwald JE, Fine SL, Jaffe GJ. Ranibizumab and bevacizumab for neovascular age-related macular degeneration. N Engl J Med 2011; 364:1897-908. [PMID: 21526923].
4. Schmidt-Erfurth U, Eldem B, Guymer R, Korobelnik JF, Schlingemann RO, Axer-Siegel R, Wiedemann P, Simader C, Gekkieva M, Weichselberger A. Efficacy and safety of monthly versus quarterly ranibizumab treatment in neovascular age-related macular degeneration: the EXCITE study. Ophthalmology 2011; 118:831-9. [PMID: 21146229].
5. Bloch SB, la Cour M, Sander B, Hansen LK, Fuchs J, Lund-Andersen H, Larsen M. Predictors of 1-year visual outcome in neovascular age-related macular degeneration following

intravitreal ranibizumab treatment. Acta ophthalmologica 2013; 91:42-7. [PMID: 22008284].

6. Rosenfeld PJ, Shapiro H, Tuomi L, Webster M, Elledge J, Blodi B. Characteristics of patients losing vision after 2 years of monthly dosing in the phase III ranibizumab clinical trials. Ophthalmology 2011; 118:523-30. [PMID: 20920825].

7. Daniel E, Toth CA, Grunwald JE, Jaffe GJ, Martin DF, Fine SL, Huang J, Ying GS, Hagstrom SA, Winter K, Maguire MG. Risk of scar in the comparison of age-related macular degeneration treatments trials. Ophthalmology 2014; 121:656-66. [PMID: 24314839].

8. Wynn TA. Common and unique mechanisms regulate fibrosis in various fibroproliferative diseases. J Clin Invest 2007; 117:524-9. [PMID: 17332879].

9. Kent D, Sheridan C. Choroidal neovascularization: a wound healing perspective. Mol Vis 2003; 9:747-55. [PMID: 14735062].

10. Kalluri R, Weinberg RA. The basics of epithelial-mesenchymal transition. J Clin Invest 2009; 119:1420-8. [PMID: 19487818].

11. Strauss O. The retinal pigment epithelium in visual function. Physiol Rev 2005; 85:845-81. [PMID: 15987797].

12. Binder S, Stanzel BV, Krebs I, Glittenberg C. Transplantation of the RPE in AMD. Prog Retin Eye Res 2007; 26:516-54. [PMID: 17532250].

13. Grisanti S, Guidry C. Transdifferentiation of retinal pigment epithelial cells from epithelial to mesenchymal phenotype. Invest Ophthalmol Vis Sci 1995; 36:391-405. [PMID: 7531185].

14. De Falco S. The discovery of placenta growth factor and its biological activity. Exp Mol Med 2012; 44:1-9. [PMID: 22228176].

15. Papadopoulos N, Martin J, Ruan Q, Rafique A, Rosconi MP, Shi E, Pyles EA, Yancopoulos GD, Stahl N, Wiegand SJ. Binding and neutralization of vascular endothelial growth factor (VEGF) and related ligands by VEGF Trap, ranibizumab and bevacizumab. Angiogenesis 2012; 15:171-85. [PMID: 22302382].

16. Chen X, Li J, Li M, Zeng M, Li T, Xiao W, Li J, Wu Q, Ke X, Luo D, Tang S, Luo Y. KH902 suppresses high glucose-induced migration and sprouting of human retinal endothelial cells by blocking VEGF and PIGF. Diabetes Obes Metab 2013; 15:224-33. [PMID: 22958404].

17. Autiero M, Waltenberger J, Communi D, Kranz A, Moons L, Lambrechts D, Kroll J, Plaisance S, De Mol M, Bono F, Kliche S, Fellbrich G, Ballmer-Hofer K, Maglione D, Mayr-Beyrle U, Dewerchin M, Dombrowski S, Stanimirovic D, Van Hummelen P, Dehio C, Hicklin DJ, Persico G, Herbert JM, Communi D, Shibuya M, Collen D, Conway EM, Carmeliet P. Role of PlGF in the intra- and intermolecular cross talk between the VEGF receptors Flt1 and Flk1. Nat Med 2003; 9:936-43. [PMID: 12796773].

18. Carmeliet P, Moons L, Luttun A, Vincenti V, Compernolle V, De Mol M, Wu Y, Bono F, Devy L, Beck H, Scholz D, Acker T, DiPalma T, Dewerchin M, Noel A, Stalmans I, Barra A, Blacher S, VandenDriessche T, Ponten A, Eriksson U, Plate KH, Foidart JM, Schaper W, Charnock-Jones DS, Hicklin DJ, Herbert JM, Collen D, Persico MG. Synergism between vascular endothelial growth factor and placental growth factor contributes to angiogenesis and plasma extravasation in pathological conditions. Nat Med 2001; 7:575-83. [PMID: 11329059].

19. Fischer C, Jonckx B, Mazzone M, Zacchigna S, Loges S, Pattarini L, Chorianopoulos E, Liesenborghs L, Koch M, De Mol M, Autiero M, Wyns S, Plaisance S, Moons L, van Rooijen N, Giacca M, Stassen JM, Dewerchin M, Collen D, Carmeliet P. Anti-PlGF inhibits growth of VEGF(R)-inhibitor-resistant tumors without affecting healthy vessels. Cell 2007; 131:463-75. [PMID: 17981115].

20. Schmidt T, Carmeliet P. Angiogenesis: a target in solid tumors, also in leukemia? Hematology (Am Soc Hematol Educ Program) 2011; 2011:1-8. [PMID: 22160005].

21. Tammela T, Enholm B, Alitalo K, Paavonen K. The biology of vascular endothelial growth factors. Cardiovasc Res 2005; 65:550-63. [PMID: 15664381].

22. Freitas-Andrade M, Carmeliet P, Charlebois C, Stanimirovic DB, Moreno MJ. PlGF knockout delays brain vessel growth and maturation upon systemic hypoxic challenge. J Cereb Blood Flow Metab (Nihongoban) 2012; 32:663-75. [PMID: 22126916].

23. Rakic JM, Lambert V, Devy L, Luttun A, Carmeliet P, Claes C, Nguyen L, Foidart JM, Noel A, Munaut C. Placental growth factor, a member of the VEGF family, contributes to the development of choroidal neovascularization. Invest Ophthalmol Vis Sci 2003; 44:3186-93. [PMID: 12824270].

24. Van de Veire S, Stalmans I, Heindryckx F, Oura H, Tijeras-Raballand A, Schmidt T, Loges S, Albrecht I, Jonckx B, Vinckier S, Van Steenkiste C, Tugues S, Rolny C, De Mol M, Dettori D, Hainaud P, Coenegrachts L, Contreres JO, Van Bergen T, Cuervo H, Xiao WH, Le Henaff C, Buysschaert I, Kharabi Masouleh B, Geerts A, Schomber T, Bonnin P, Lambert V, Haustraete J, Zacchigna S, Rakic JM, Jimenez W, Noel A, Giacca M, Colle I, Foidart JM, Tobelem G, Morales-Ruiz M, Vilar J, Maxwell P, Vinores SA, Carmeliet G, Dewerchin M, Claesson-Welsh L, Dupuy E, Van Vlierberghe H, Christofori G, Mazzone M, Detmar M, Collen D, Carmeliet P. Further pharmacological and genetic evidence for the efficacy of PlGF inhibition in cancer and eye disease. Cell 2010; 141:178-90. [PMID: 20371353].

25. Hollborn M, Reichmuth K, Prager P, Wiedemann P, Bringmann A, Kohen L. Osmotic induction of placental growth factor in retinal pigment epithelial cells in vitro: contribution of NFAT5 activity. Mol Biol Rep 2016; 43:803-14. [PMID: 27230578].

26. Zhou AY, Bai YJ, Zhao M, Yu WZ, Huang LZ, Li XX. Placental growth factor expression is reversed by antivascular endothelial growth factor therapy under hypoxic conditions. World journal of pediatrics WJP 2014; 10:262-70. [PMID: 25124978].

27. Zhang L, Zhao S, Yuan L, Wu H, Jiang H, Luo G. Placenta growth factor contributes to cell apoptosis and epithelial-to-mesenchymal transition in the hyperoxia-induced acute lung injury. Life Sci 2016; 156:30-7. [PMID: 27211521].

28. Zhang L, Zhao S, Yuan L, Wu H, Jiang H, Luo G. Placental Growth Factor Triggers Epithelial-to-Mesenchymal Transition-like Changes in Rat Type II Alveolar Epithelial Cells: Activation of Nuclear Factor kappaB Signalling Pathway. Basic Clin Pharmacol Toxicol 2016; 119:498-504. [PMID: 27154788].

29. Huang W, Zhu S, Liu Q, Li C, Li L. Placenta growth factor promotes migration through regulating epithelial-mesenchymal transition-related protein expression in cervical cancer. Int J Clin Exp Pathol 2014; 7:8506-19. [PMID: 25674215].

30. Ning Q, Liu C, Hou L, Meng M, Zhang X, Luo M, Shao S, Zuo X, Zhao X. Vascular endothelial growth factor receptor-1 activation promotes migration and invasion of breast cancer cells through epithelial-mesenchymal transition. PLoS One 2013; 8:e65217-[PMID: 23776453].

31. Mammadzada P, Gudmundsson J, Kvanta A, Andre H. Differential hypoxic response of human choroidal and retinal endothelial cells proposes tissue heterogeneity of ocular angiogenesis. Acta ophthalmologica 2016; 94:805-14. [PMID: 27255568].

32. Klaassen I, de Vries EW, Vogels IMC, van Kampen AHC, Bosscha MI, Steel DHW, Van Noorden CJF, Lesnik-Oberstein SY, Schlingemann RO. Identification of proteins associated with clinical and pathological features of proliferative diabetic retinopathy in vitreous and fibrovascular membranes. PLoS One 2017; 12:e0187304-[PMID: 29095861].

33. Xu XH, Zhao C, Peng Q, Xie P, Liu QH. Kaempferol inhibited VEGF and PGF expression and in vitro angiogenesis of HRECs under diabetic-like environment. Brazilian journal of medical and biological research = Rev Bras Pesqui Med Biol 2017; 50:e5396-[PMID: 28273207].

34. Huang H, Parlier R, Shen JK, Lutty GA, Vinores SA. VEGF receptor blockade markedly reduces retinal microglia/macrophage infiltration into laser-induced CNV. PLoS One 2013; 8:e71808-[PMID: 23977149].

35. Crespo-Garcia S, Corkhill C, Roubeix C, Davids AM, Kociok N, Strauss O, Joussen AM, Reichhart N. Inhibition of Placenta Growth Factor Reduces Subretinal Mononuclear Phagocyte Accumulation in Choroidal Neovascularization. Invest Ophthalmol Vis Sci 2017; 58:4997-5006. [PMID: 28979997].

36. Ogura S, Kurata K, Hattori Y, Takase H, Ishiguro-Oonuma T, Hwang Y, Ahn S, Park I, Ikeda W, Kusuhara S, Fukushima Y, Nara H, Sakai H, Fujiwara T, Matsushita J, Ema M, Hirashima M, Minami T, Shibuya M, Takakura N, Kim P, Miyata T, Ogura Y, Uemura A. Sustained inflammation after pericyte depletion induces irreversible blood-retina barrier breakdown. JCI Insight 2017; 2:e90905-[PMID: 28194443].

37. Kernt M, Liegl RG, Rueping J, Neubauer AS, Haritoglou C, Lackerbauer CA, Eibl KH, Ulbig MW, Kampik A. Sorafenib protects human optic nerve head astrocytes from light-induced overexpression of vascular endothelial growth factor, platelet-derived growth factor, and placenta growth factor. Growth Factors 2010; 28:211-20. [PMID: 20166888].

38. Hollborn M, Tenckhoff S, Seifert M, Kohler S, Wiedemann P, Bringmann A, Kohen L. Human retinal epithelium produces and responds to placenta growth factor. Graefe's archive for clinical and experimental ophthalmology = Albrecht Von Graefes Arch Klin Exp Ophthalmol 2006; 244:732-41. .

39. Akrami H, Soheili ZS, Sadeghizadeh M, Ahmadieh H, Rezaeikanavi M, Samiei S, Khalooghi K. PlGF gene knockdown in human retinal pigment epithelial cells. Graefe's archive for clinical and experimental ophthalmology = Albrecht Von Graefes Arch Klin Exp Ophthalmol 2011; 249:537-46. .

40. Michels S, Schmidt-Erfurth U, Rosenfeld PJ. Promising new treatments for neovascular age-related macular degeneration. Expert Opin Investig Drugs 2006; 15:779-93. [PMID: 16787141].

41. Thomson S, Petti F, Sujka-Kwok I, Mercado P, Bean J, Monaghan M, Seymour SL, Argast GM, Epstein DM, Haley JD. A systems view of epithelial-mesenchymal transition signaling states. Clin Exp Metastasis 2011; 28:137-55. [PMID: 21194007].

42. Kriz W, Kaissling B, Le Hir M. Epithelial-mesenchymal transition (EMT) in kidney fibrosis: fact or fantasy? J Clin Invest 2011; 121:468-74. [PMID: 21370523].

43. O'Connor JW, Gomez EW. Biomechanics of TGFbeta-induced epithelial-mesenchymal transition: implications for fibrosis and cancer. Clin Transl Med 2014; 3:23-[PMID: 25097726].

44. Pereira TN, Walsh MJ, Lewindon PJ, Ramm GA. Paediatric cholestatic liver disease: Diagnosis, assessment of disease progression and mechanisms of fibrogenesis. World J Gastrointest Pathophysiol 2010; 1:69-84. [PMID: 21607144].

45. Lamouille S, Xu J, Derynck R. Molecular mechanisms of epithelial-mesenchymal transition. Nat Rev Mol Cell Biol 2014; 15:178-96. [PMID: 24556840].

46. Chen Y, Ge W, Xu L, Qu C, Zhu M, Zhang W, Xiao Y. miR-200b is involved in intestinal fibrosis of Crohn's disease. Int J Mol Med 2012; 29:601-6. [PMID: 22294131].

47. Bai F, Huang Q, Wei J, Lv S, Chen Y, Liang C, Wei L, Lu Z, Lin X. Gypsophila elegans isoorientin-2''-O-alpha-l-arabinopyranosyl ameliorates porcine serum-induced immune liver fibrosis by inhibiting NF-kappaB signaling pathway and suppressing HSC activation. Int Immunopharmacol 2017; 54:60-7. [PMID: 29107862].

48. Liu H, Xiong J, He T, Xiao T, Li Y, Yu Y, Huang Y, Xu X, Huang Y, Zhang J, Zhang B, Zhao J. High Uric Acid-Induced Epithelial-Mesenchymal Transition of Renal Tubular Epithelial Cells via the TLR4/NF-kB Signaling Pathway. Am J Nephrol 2017; 46:333-42. [PMID: 29017152].

49. Hou J, Ma T, Cao H, Chen Y, Wang C, Chen X, Xiang Z, Han X. TNF-α-induced NF-κB activation promotes myofibroblast

differentiation of LR-MSCs and exacerbates bleomycin-induced pulmonary fibrosis. J Cell Physiol 2018; 233:2409-19. [PMID: 28731277].

50. Kim KH, Lee WR, Kang YN, Chang YC, Park KK. Inhibitory effect of nuclear factor-kappaB decoy oligodeoxynucleotide on liver fibrosis through regulation of the epithelial-mesenchymal transition. Hum Gene Ther 2014; 25:721-9. [PMID: 24959740].

51. Li M, Hu L, Zhu F, Zhou Z, Tian J, Ai J. Hepatitis B virus X protein promotes renal epithelial-mesenchymal transition in human renal proximal tubule epithelial cells through the activation of NF-kappaB. Int J Mol Med 2016; 38:513-20. [PMID: 27314843].

52. Tamiya S, Liu L, Kaplan HJ. Epithelial-mesenchymal transition and proliferation of retinal pigment epithelial cells initiated upon loss of cell-cell contact. Invest Ophthalmol Vis Sci 2010; 51:2755-63. [PMID: 20042656].

Articles are provided courtesy of Emory University and the Zhongshan Ophthalmic Center, Sun Yat-sen University, P.R. China. The print version of this article was created on 26 April 2018. This reflects all typographical corrections and errata to the article through that date. Details of any changes may be found in the online version of the article.